

Spatial radionuclide deposition data from the 60 km radial area around the Chernobyl nuclear power plant: results from a sampling survey in 1987

Valery Kashparov^{1,3}, Sviatoslav Levchuk¹, Marina Zhurba¹, Valentyn Protsak¹, Nicholas A. Beresford², and Jacqueline S. Chaplow²

¹ Ukrainian Institute of Agricultural Radiology of National University of Life and Environmental Sciences of Ukraine, Mashinobudivnykiv str.7, Chabany, Kyiv region, 08162 Ukraine

² UK Centre for Ecology & Hydrology, Lancaster Environment Centre, Library Avenue, Bailrigg, Lancaster, LA1 4AP, UK

³ CERAD CoE Environmental Radioactivity/Department of Environmental Sciences, Norwegian University of Life Sciences, 1432 Aas, Norway

Correspondence to: Jacqueline S. Chaplow (jgar@ceh.ac.uk)

Abstract. The data set “Spatial radionuclide deposition data from the 60 radial km area around the Chernobyl nuclear power plant: results from a sampling survey in 1987” is the latest in a series of data to be published by the Environmental Information Data Centre (EIDC) describing samples collected and analysed following the Chernobyl nuclear power plant accident in 1986. The data result from a survey carried out by the Ukrainian Institute of Agricultural Radiology (UIAR) in April and May 1987 and include sample site information, dose rate, radionuclide (zirconium-95, niobium-95, ruthenium-106, caesium-134, caesium-137 and cerium-144) deposition, and exchangeable (determined following 1M NH₄Ac extraction of soils) caesium-134 and 137.

The purpose of this paper is to describe the available data and methodology used for sample collection, sample preparation, and analysis. The data will be useful in the reconstruction of doses to human and wildlife populations, answering the current lack of scientific consensus on the effects of radiation on wildlife in the Chernobyl Exclusion zone and in evaluating future management options for Chernobyl impacted area of Ukraine and Belarus.

The data and supporting documentation are freely available from the Environmental Information Data Centre (EIDC) under the terms and conditions of the Open Government Licence (Kashparov et al., 2019 <https://doi.org/10.5285/a408ac9d-763e-4f4c-ba72-73bc2d1f596d>).

1 Background

The dynamics of the releases of radioactive substance from the number four reactor at the Chernobyl nuclear power plant (ChNPP) and meteorological conditions over the ten days following the accident on the 26th April 1986 resulted in a complex pattern of contamination over most of Europe (IAEA, 2006).

The neutron flux rise and a sharp increase in energy emission at the time of the accident resulted in heating of the nuclear fuel and leakage of fission products. Destruction of the fuel rods caused an increase in heat transfer to the surface of the superheated fuel particles and coolant, and release of radioactive substances into the atmosphere (Kashparov et al., 1996). According to the latest estimates (Kashparov et al., 2003; UNSCEAR, 2008) 100% of inert radioactive gases (largely ⁸⁵Kr and ¹³³Xe), 20-60% of iodine isotopes, 12-40% of ^{134,137}Cs and 1.4-4% of less volatile radionuclides (⁹⁵Zr, ⁹⁹Mo, ^{89,90}Sr, ^{103,106}Ru, ^{141,144}Ce, ^{154,155}Eu, ²³⁸⁻²⁴¹Pu etc.) in the reactor at the moment of the accident were released to the atmosphere.

As a result of the initial explosion on 26th April 1986, a narrow (100 km long and up to 1 km wide) relatively straight trace of radioactive fallout formed to the west of the reactor in the direction of Red Forest and Tolsty Les village (this has subsequently become known as the

47 ‘western trace’). This trace was mainly finely dispersed nuclear fuel (Kashparov et al., 2003,
48 2018) and could only have been formed as a consequence of the short-term release of fuel
49 particles with overheated vapour to a comparatively low height during night time (the accident
50 occurred at 01:24) stable atmospheric conditions. At the time of the accident, surface winds
51 were weak and did not have any particular direction; only at a height of 1500 m was there a
52 south-western wind with the velocity 8-10 m·s⁻¹ (IAEA, 1992). Cooling of the release cloud,
53 which included steam, resulted in the decrease of its volume, water condensation and wet
54 deposition of radionuclides as mist (as the released steam cooled) (Saji, 2005). Later, the main
55 mechanism of fuel particle formation was the oxidation of the nuclear fuel (Kashparov et al.,
56 1996; Salbu et al., 1994). There was an absence of data on meteorological conditions in the
57 area of ChNPP at the time of the accident (the closest observations were more than 100 km
58 away to the west (Izrael et al., 1990)). There was also a lack of source term information and
59 data on the composition of dispersed radioactive fallout. Consequently, it was not possible to
60 make accurate predictions of deposition for the area close to the ChNPP (Talerko, 2005).

61 The relative leakage of fission products of uranium (IV) oxide in an inert environment at
62 temperatures up to 2600 °C decreases in the order: volatile (Xe, Kr, I, Cs, Te, Sb, Ag), semi-
63 volatile (Mo, Ba, Rh, Pd, Tc) and nonvolatile (Sr, Y, Nb, Ru, La, Ce, Eu) (Kashparov et al.,
64 1996; Pontillon et al., 2010). As a result of the estimated potential remaining heat release from
65 fuel at the time of the accident (~230 W kg⁻¹ U) and the heat accumulation in fuel (National
66 Report of Ukraine, 2011), highly mobile volatile fission products (Kr, Xe, iodine, tellurium,
67 caesium) were released from the fuel of the reactor and raised to a height of more than 1 km
68 on 26th April 1986 and to approximately 600 m over the following days (IAEA, 1992; Izrael et
69 al., 1990). The greatest release of radiocaesium occurred during the period of maximum heating
70 of the reactor fuel on 26-28th April 1986 (Izrael et al., 1990). This caused the formation of the
71 western, south-western (towards the settlements of Poliske and Bober), north-western
72 (ultimately spreading to Sweden and wider areas of western Europe), and north-eastern
73 condensed radioactive traces. Caesium deposition at distances from Chernobyl was largely
74 determined by the degree of precipitation (e.g. see Chaplow et al. (2015) discussing deposition
75 across Great Britain). After the covering of the reactor by dropping materials (including 40 t
76 of boron carbide, 2500 t of lead, 1800 t of sand and clay, 800 t of dolomite) from helicopters
77 over the period 27th April–10th May 1986 (National Report of Ukraine, 2011), the ability for
78 heat exchange of the fuel reduced, which caused a rise of temperature and consequent increase
79 of the leakage of volatile fission products and the melting of the materials which had been
80 dropped onto the reactor. Subsequently, there was a sharp reduction in the releases of
81 radionuclides from the destroyed reactor on 6th May 1986 (National Report of Ukraine, 2011)
82 due to aluminosilicates forming thermally stable compounds with many fission products and
83 fixing caesium and strontium at high temperature (a process known prior to the Chernobyl
84 accident (Hilpert & Nurberg, 1983)).

85 The changes of the annealing temperature of the nuclear fuel during the accident had a strong
86 effect on both the ratio of different volatile fission products released (the migratory properties
87 of Xe, Kr, I, Te, Cs increased with the temperature rise and were influenced by the presence of
88 UO₂) and the rate of destruction of the nuclear fuel which oxidised forming micronized fuel
89 particles (Salbu et al., 1994; Kashparov et al., 1996). The deposition of radionuclides such as
90 ⁹⁰Sr, ²³⁸⁻²⁴¹Pu, ²⁴¹Am, which were associated with the fuel component of the Chernobyl releases
91 was largely limited to areas relatively close to the ChNPP. Areas receiving deposition of these

92 radionuclides were the Chernobyl Exclusion Zone (i.e. the area of approximately 30 km radius
93 around the ChNPP), and adjacent territories in the north of the Kiev region, in the west of the
94 Chernihiv region, and the Bragin and Hoyniki districts of the Gomel region (Belarus).
95 Deposition was related to the rate of the dry gravitational sedimentation of the fuel particles
96 caused by their high density (about 8-10 g·cm⁻³ (Kashparov et al., 1996)); sedimentation of the
97 lightweight condensation particles, containing iodine and caesium radioisotopes, was lower
98 and hence these were transported further.

99 After the Chernobyl accident, western Europe and the Ukrainian-Belorussian Polesye were
100 contaminated with radionuclides (IAEA, 1991, 1992, 2006). However, the area extending to
101 60-km around the ChNPP was the most contaminated (Izrael et al., 1990). Work on the
102 assessment of the radiological situation within the zone started within a few days of the
103 accident; the aim of this work was the radiation protection of the population and personnel.
104 Subsequently, further quantification of terrestrial dose rates was carried out by aerial-gamma
105 survey by the State Hydrometeorological Committee together with Ministry of Geology and
106 Ministry of Defence of USSR (as reported in Izrael et al., 1990). Large-scale sampling of soil
107 was also conducted, with samples analysed using gamma-spectrometry and radiochemistry
108 methods (see Izrael et al., 1990). These studies showed high variability in dose rates and
109 radionuclide activity concentrations, with spatial patterns in both radioactive contamination
110 and the radionuclide composition of fallout (Izrael et al., 1990).

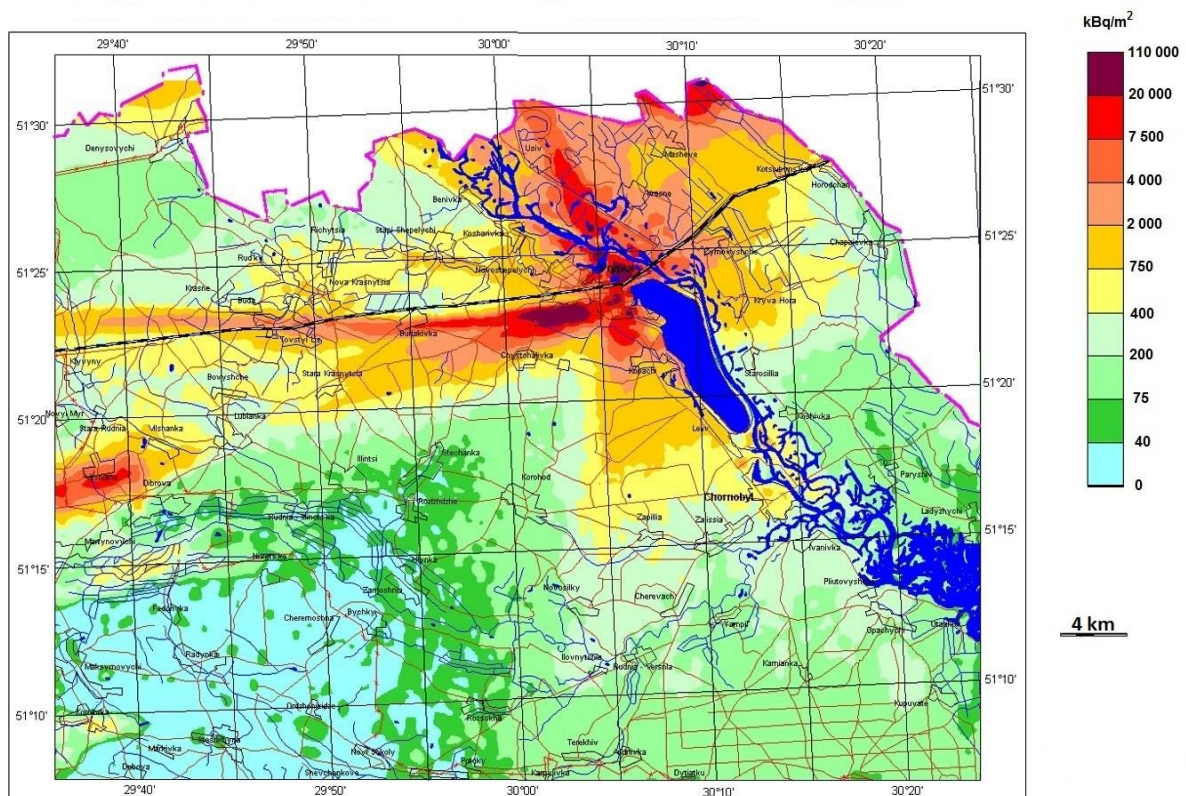
111 The initial area from which the population was evacuated was based on an arbitrary decision
112 whereby a circle around the Chernobyl nuclear power plant with a radius of 30 km was defined
113 (IAEA, 1991). In the initial phase after the accident (before 7th May 1986) 99195 people were
114 evacuated from 113 settlements including 11358 people from 51 villages in Belarus and 87 837
115 people from 62 settlements in Ukraine (including about 45 thousand people evacuated between
116 14.00-17.00 hours on April 27 from the town of Pripjat located 4 km from the ChNPP)
117 (Aleksakhin et al., 2001).

118 The analysis of data available in May 1986 showed that the extent of the territory with
119 radioactive contamination where comprehensive measures were required to protect the
120 population extended far beyond the 30 km Chernobyl Exclusion Zone (CEZ). A temporary
121 annual effective dose limit of 100 mSv for the period from 26th April 1986 to 25th April 1987
122 (50 mSv from external and 50 mSv from internal exposure) was set by the USSR Ministry of
123 Health. To identify areas outside of the CEZ where the population required evacuation, dose
124 criteria had to be defined. It was proposed to use the average value of the dose rate of gamma
125 radiation in open air for an area (estimated for 10th May 1986) to help define an evacuation
126 zone. An exposure dose rate of 5 mR h⁻¹ estimated for 10th May 1986 (approximating to an
127 effective dose rate (EDR) of gamma radiation in air of 50 μSv h⁻¹) equated to an external annual
128 dose of 50 mSv for the period from 26th April 1986 to 25th April 1987.

129 At the end of May 1986 an approach to identify areas where evacuation was required using
130 estimated internal dose rates was proposed. This used the average density of the surface
131 contamination of the soil with long-lived biologically significant nuclides (¹³⁷Cs, ⁹⁰Sr, ^{239,240}Pu)
132 in a settlement and modelling to estimate the contamination of foodstuffs and hence diet. The
133 numerical values suggested to identify areas for evacuation were: 15 Ci km⁻² (555 kBq m⁻²) of
134 ¹³⁷Cs, 3 Ci km⁻² (111 kBq m⁻²) of ⁹⁰Sr and 0.1 Ci km⁻² (3.7 kBq m⁻²) of ^{239,240}Pu; this equated
135 to an internal dose of 50 mSv over the first year after the accident.

136 However, in reality the main criterion for the evacuation was the exposure dose rate ($R\ h^{-1}$) and
137 where the exposure dose rate exceeded $5\ mR\ h^{-1}$ (EDR in air of about $50\ \mu Sv\ h^{-1}$) the evacuated
138 population were not allowed to return.

139 Hence, in 1986 the boundary of the population evacuation zone was set at an exposure dose
140 rate of $5\ mR\ h^{-1}$ (EDR of about $50\ \mu Sv\ h^{-1}$). However, the ratio of short-lived gamma-emitting
141 radionuclides (^{95}Zr , ^{95}Nb , ^{106}Ru , ^{144}Ce) deposited as fuel particles to $^{134,137}Cs$ deposited as
142 condensation particles, was inconsistent across the evacuated areas. Therefore, after the
143 radioactive decay of the short-lived radionuclides the residual dose rate across the evacuated
144 areas varied considerably and was largely determined by the pattern of long-lived ^{137}Cs
145 deposition (e.g. Figure 1) (Kashparov et al., 2018).



146
147 Figure 1. Caesium-137 deposition in the Ukrainian 30 km exclusion zone estimated for 1997
148 (from UIAR, 1998).

149
150 The first measurements of activity concentration of radionuclides in soil showed that
151 radionuclide activity concentration ratios depended on distance and direction from the ChNPP
152 (Izrael et al., 1990). Subsequent to this observation a detailed study of soil contamination was
153 started in 1987 (Izrael et al., 1990). Taking into account the considerable heterogeneity of
154 terrestrial contamination with radioactive substances in a large area, sampling along the
155 western, southern and northern traces was carried out in stages finishing in 1988.

156 In 1987 the State Committee of Hydrometeorology of the USSR and the Scientific Centre of
157 the Defence Ministry of the USSR established a survey programme to monitor radionuclide
158 activity concentrations in soil. For this purpose, 540 sampling sites were identified at a distance
159 of 5 km to 60 km around the ChNPP using a polar coordinate system centred on the ChNPP.
160 Fifteen sampling sites were selected on each of the 36 rays drawn every 10 degrees (Loshchilov

161 et al., 1991) (Figures 3 and 4). Radionuclide activity concentrations in soil samples collected
162 on the radial network were determined by the UIAR and used to calculate the radionuclide
163 contamination density. These data are discussed in this paper and the full data set is freely
164 available from Kashparov et al. (2019).

165

166 **2 Data**

167 The data (Kashparov et al., 2019) include location of sample sites (angle and distance from the
168 ChNPP), dose rate, radionuclide deposition data, counting efficiency and information on
169 exchangeable ^{134,137}Cs.

170 The data are presented in a table with 21 columns and 540 rows of data (plus column headings)
171 as one Microsoft Excel Comma Separated Value File (.csv) as per the requirements of the
172 Environmental Information Data Centre. Appendix 1 presents an explanation of the column
173 headings and units used in the data (Kashparov et al., 2019).

174

175 **2.1 Sampling**

176 To enable long-term monitoring and contamination mapping of the 60 km zone around the
177 ChNPP, 540 points were defined and sampled in April – May 1987. The sampling strategy
178 used a radial network with points at every 10° (from 10° to 360°); sampling points were located
179 at distances of 5 km, 6 km, 7 km, 8.3 km, 10 km, 12 km, 14.7 km, 17 km, 20 km, 25 km, 30
180 km, 37.5 km, 45 km, 52.5 km and 60 km (Figures 3 and 4). The locations of sampling points
181 were identified using military maps (1:10000 scale) and local landscape. Sampling sites
182 (identified using an index post) were estimated to be within 10 m of distances and directions
183 as recorded in the accompanying data set. Sites were resampled regularly until 1990 and
184 sporadically thereafter, however, data for these subsequent samplings are not reported here as
185 they are unavailable (including to the UIAR).

186 Samples were not collected from points located in swamps, rivers and lakes; in total 489
187 samples were collected. A corer with a diameter of 14 cm was used to collect soil samples
188 down to a depth of 5 cm from five points at each location using the envelope method (with
189 approximately 5-10 m between sampling points) (Figure 2) (Loshchilov et al., 1991). Soil cores
190 were retained intact during transportation to the laboratory. At each sampling point, the
191 exposure dose rate was determined 1 m above ground level.

192

193



194
195

196 Figure 2. Soil sampling using a ring of 14 cm diameter to collect a 5 cm deep soil core (courtesy
197 of UIAR, 1989).

198

199 2.2 Analysis

200 Using a high-purity germanium detector (GEM-30185, ORTEC, USA) and a multichannel
201 analyser “ADCAM-300” (ORTEC, USA), the activity concentration of gamma emitting
202 radionuclides (zirconium-95 (^{95}Zr), niobium-95 (^{95}Nb), ruthenium-106 (^{106}Ru), caesium-134
203 (^{134}Cs), caesium-137, (^{137}Cs) cerium-144 (^{144}Ce)) was determined in one soil sample from each
204 sampling site. Information on gamma lines used in the analyses and radioisotope half-lives
205 assumed for decay correction are presented in Appendix 2. Soil samples were analysed in a 1
206 litre Marinelli container. The other four cores were sent to different laboratories in the Soviet
207 Union (data for these cores are unfortunately not available). Using a 1M NH_4Ac solution (pH
208 7) a 100 g subsample of soil was leached (solid: liquid ratio 1:5). The resultant leachate solution
209 was shaken for 1 hour and then left at room temperature for 1 day before filtering through
210 ashless filter paper (3-5 μm). The filtrate was then put into a suitable container for gamma
211 analysis to determine the fraction of exchangeable $^{134,137}\text{Cs}$. Measured activity concentrations
212 were reported at 68% confidence level (which equates to one standard deviation).

213 Decay radiation information from the master library, integrated in spectrum analysing software
214 tool Gelicam (EG&G ORTEC, USA), was used in gamma-analyses. Activities of ^{106}Ru and
215 ^{137}Cs in samples were estimated via their gamma radiation emitting progenies ^{106}Rh and $^{137\text{m}}\text{Ba}$,
216 respectively.

217

218 Calibration of the spectrometer was conducted using certified standards (soil equivalent multi-
219 radionuclide standard, V. G. Khlopin Radium Institute, Russia). Quality assurance/quality
220 control procedures included regular monitoring of the system performance, efficiency,
221 background and full width at half maximum (FWHM) for the ^{144}Ce , ^{137}Cs and ^{95}Nb photo
222 peaks. To validate accuracy and precision of the method employed for ^{137}Cs activity
223 concentration measurements, quality control samples (i.e., different matrix samples including
224 water, soil and sawdust spiked with known certified activities of radionuclides) and Certified
225 Reference Materials (CRM) were analysed alongside the samples. Analysis of IAEA CRMs
226 showed satisfactory results for radionuclide mean activity concentrations with results being
227 within the 95% confidence interval; the limit of detection for ^{137}Cs in all samples was 1 Bq.

228 Subsamples were analysed in a different laboratory (USSR Ministry of Defence) and results
229 for the two laboratories were within the error of determination.

230 The density of soil contamination (Bq m^{-2}) was calculated from the estimated radionuclide
231 activity concentrations in soils. It has been estimated that uncertainty from using a single soil
232 sample (of area 0.015 m^2) to estimate the value of contamination density of a sampling site (the
233 area from which five cores were collected) may be up to 50% (IAEA, 2019).

234

235 The data described in this paper (Kashparov et al., 2020) comprise exposure dose rate (mR/h),
236 date of gamma activity measurement, density of contamination (Bq m^{-2}) of ^{95}Zr , ^{95}Nb , ^{106}Ru ,
237 ^{134}Cs , ^{137}Cs and ^{144}Ce (with associated activity measurement uncertainties) and density of
238 contamination of $^{134+137}\text{Cs}$ in exchangeable form. Reported radionuclide activity concentration
239 values are for the date of measurement (samples were analysed within 1.5 months of
240 collection).

241

242 For presentation below, radionuclide activity concentrations have been decay corrected to 6th
243 May 1986 (the date on which releases from the reactor in-effect stopped) using the equation:
244 $A_T = A_0/e^{-\lambda t}$ where A_T equals the radionuclide activity concentration at the time of measurement
245 (t); A_0 is the activity concentration on 6th May 1986, and λ is the decay constant (i.e.
246 $0.693/\text{radionuclide physical half-life}$ (see Table 1 for radionuclide half-lives)).

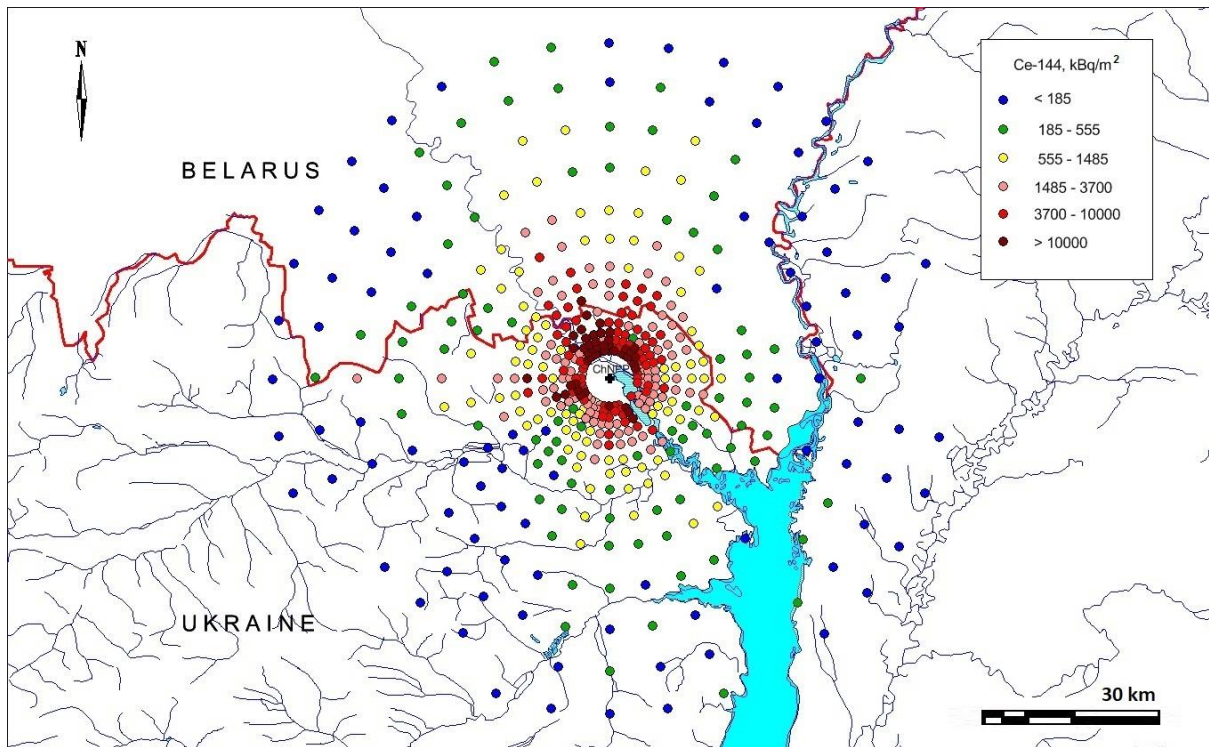
247

248 **2.3 Results**

249 The contamination density of ^{144}Ce and ^{137}Cs are presented in Figure 3 and 4; the activity
250 concentrations as presented in the figures have been decay corrected to 6th May 1986. The
251 density of ^{144}Ce contamination decreased exponentially with distance (Figures 3 and 5),
252 because ^{144}Ce was released in the fuel particles, which had a high dry deposition velocity
253 (Kuriny et al., 1993). The fallout density of ^{144}Ce decreased by 7-9 times between the 5 km and
254 30 km sampling sites, and by 70-120 times between the 5 km and 60 km sampling sites (Figure
255 5).

256

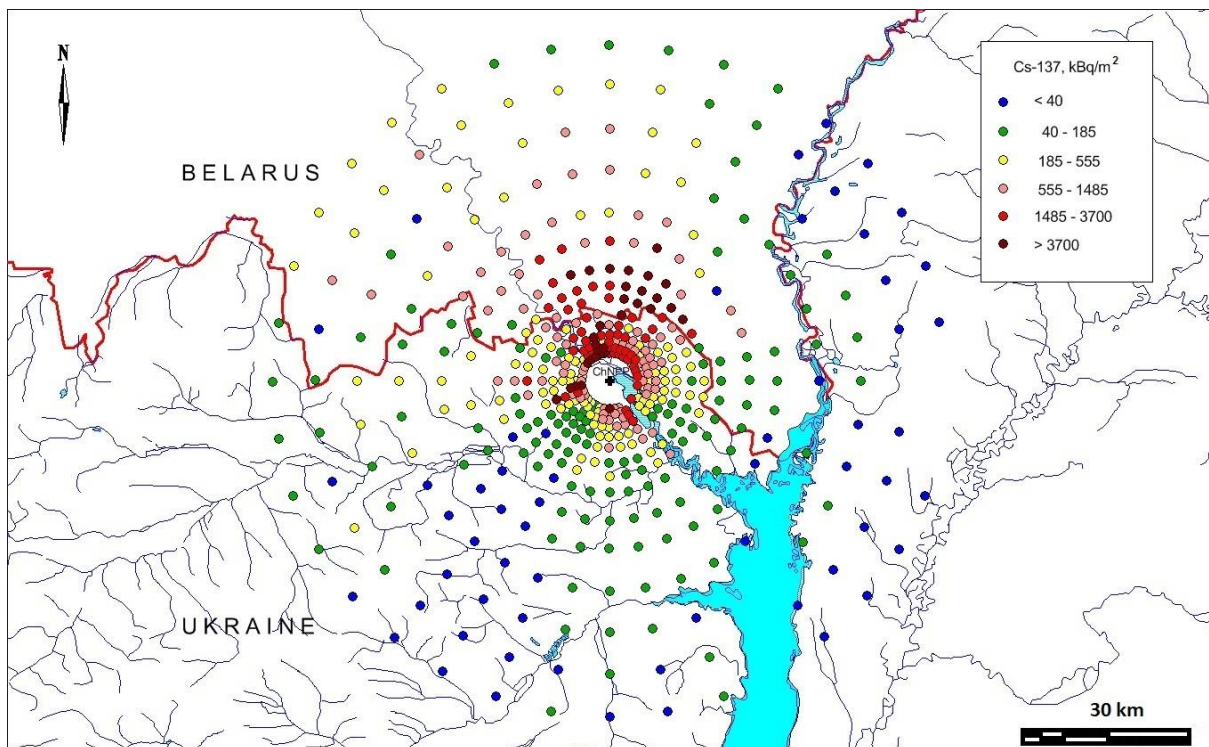
257 The fallout density of ^{137}Cs decreased similarly to that of ^{144}Ce along the southern ‘fuel trace’
258 (Figure 5a). The contamination density of ^{137}Cs along the western trace decreased less than the
259 ^{144}Ce contamination density due to the importance of the condensation component of the fallout
260 in this direction (with a resultant R^2 value for the relationship between ^{137}Cs and distance lower
261 than seen for ^{144}Ce and ^{137}Cs in different directions) (Figure 5b). The comparative decrease of
262 ^{137}Cs contamination density along the northern trace (mixed fuel and condensation fallout) was
263 in between that of the southern and western traces (Figure 5c) although there were caesium
264 hotspots in the northern condensation trace (Figures 4 and 5c). The activity ratio of ^{144}Ce to
265 ^{137}Cs decreased with distance from the ChNPP due to the condensation component being more
266 important for ^{137}Cs ; the condensation component had a lower deposition velocity compared
267 with fuel particles (with which ^{144}Ce was associated) (Figure 6). The ratio $^{144}\text{Ce}/^{137}\text{Cs}$ for
268 Chernobyl reactor fuel on 6th May 1986 can be estimated to be 15 from data presented in Table
269 1. The ratio was about 11 (geometric mean of 1167 measurements) in Chernobyl fuel particles
270 larger than $10 \mu\text{m}$ due to caesium escape during high-temperature annealing (Kuriny et al.,
271 1993). The ratio of $^{144}\text{Ce}/^{137}\text{Cs}$ in deposition exceeded five in the south-east and in the south
272 up to 60 km and 30 km from the NPP respectively (Figure 6). Thus, activities of $^{134,137}\text{Cs}$ in the
273 condensate and in the fuel components in these directions were of approximate equal
274 importance. The condensation component of caesium was more important in the north and
275 dominated in the west (Figure 8) (Loshchilov et al., 1991; Kuriny et al., 1993); the more rapidly
276 changing $^{144}\text{Ce}/^{137}\text{Cs}$ ratios in these directions are reflective of this (Figure 6).



277

278 Figure 3. The fallout density of ^{144}Ce (kBq/m^2) within the 60 km zone around the ChNPP
 279 decay corrected to 6th May 1986.

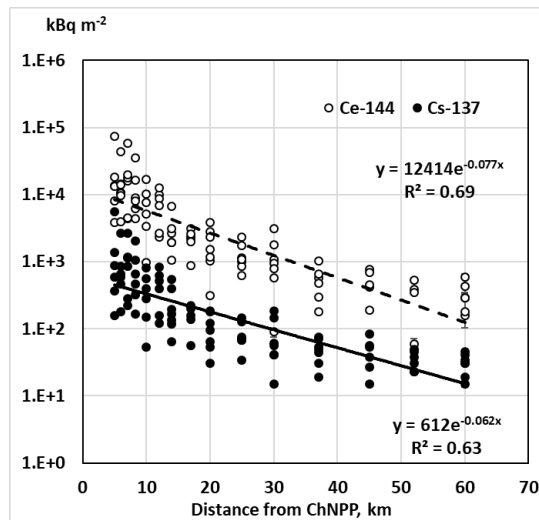
280



281

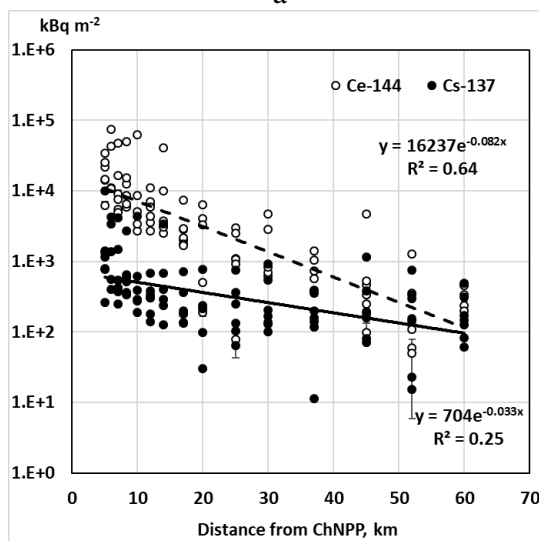
282 Figure 4. The fallout density of ^{137}Cs (kBq/m^2) within the 60 km zone around the ChNPP
 283 decay corrected to 6th May 1986.

284
285



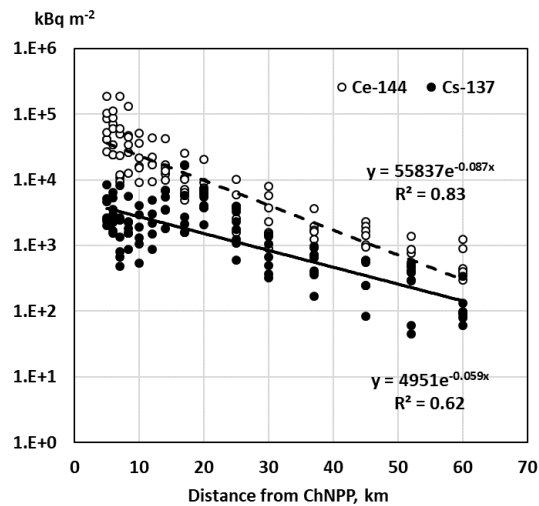
a

286
287



b

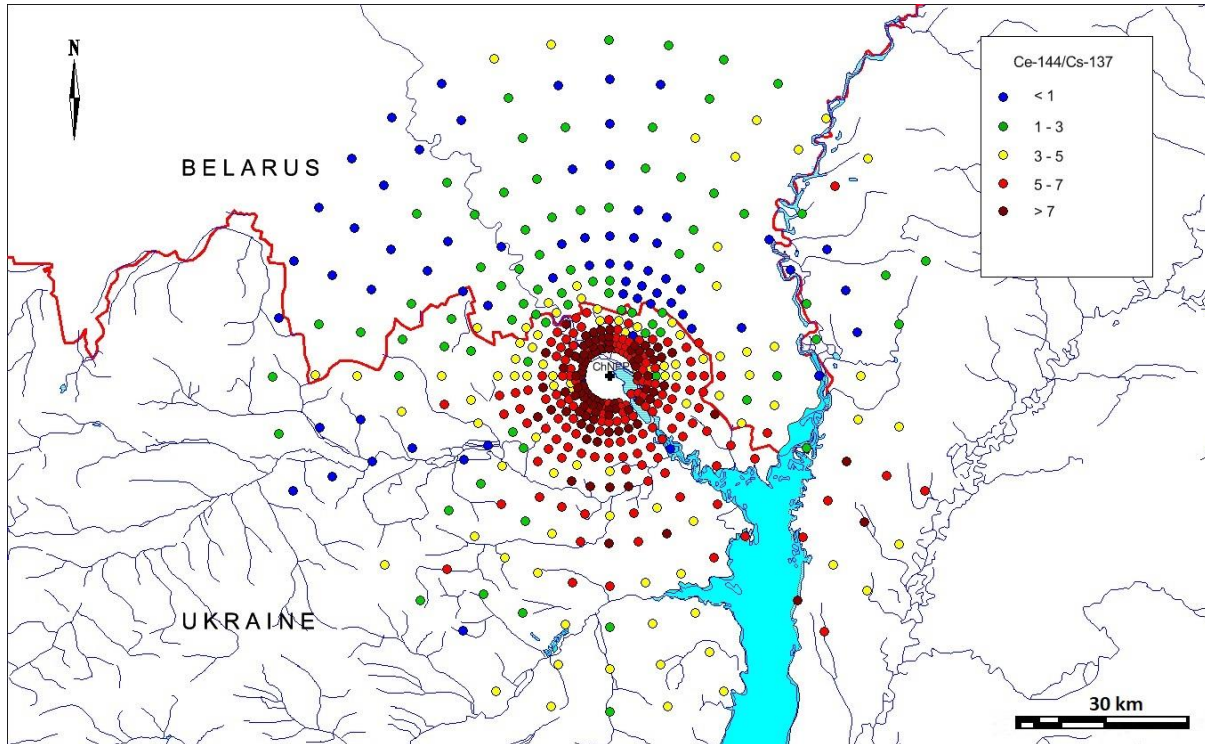
288
289
290



c

291 Figure 5. Relationship between fallout density of ¹⁴⁴Ce (1) and ¹³⁷Cs (2) and distance from
292 the ChNPP towards the south (a) (150-210°), the west (b) (240-300°) and the north (c) (330-
293 30°).

294



295

296 Figure 6. $^{144}\text{Ce}/^{137}\text{Cs}$ ratio within the 60 km zone around the ChNPP decay corrected to 6th
 297 May 1986.

298

299 Table 1. The average activity concentrations of radionuclides with half-life ($T_{1/2}$) >1 day
 300 estimated in the fuel of the ChNPP number four reactor recalculated for 6th May 1986
 301 (Begichev et al., 1993).

302

Radionuclide	Half-life (days)	Average activity concentration (Bq g ⁻¹)	Radionuclide	Half-life (days)	Average activity concentration (Bq g ⁻¹)
⁷⁵ Se	1.2 x 10 ²	5.4 x 10 ⁶	¹³² Te	3.3 x 10 ⁰	2.4 x 10 ¹⁰
⁷⁶ As	1.1 x 10 ⁰	1.7 x 10 ⁷	¹³³ Xe	5.2 x 10 ⁰	3.4 x 10 ¹⁰
⁷⁷ As	1.6 x 10 ⁰	4.1 x 10 ⁷	¹³⁴ Cs	7.6 x 10 ⁻²	8.9 x 10 ⁸
⁸² Br	1.5 x 10 ⁰	1.8 x 10 ⁹	¹³⁵ Cs	5.5 x 10 ⁷	1.9 x 10 ⁴
⁸⁵ Kr	3.9 x 10 ³	1.5 x 10 ⁸	¹³⁶ Cs	1.3 x 10 ¹	3.3 x 10 ¹⁰
⁸⁶ Rb	1.9 x 10 ¹	8.7 x 10 ⁹	¹³⁷ Cs	1.1 x 10 ⁴	1.4 x 10 ⁹
⁸⁹ Sr	5.1 x 10 ¹	2.1 x 10 ¹⁰	¹⁴⁰ Ba	1.3 x 10 ¹	3.2 x 10 ¹⁰
⁹⁰ Sr	1.1 x 10 ⁴	1.2 x 10 ⁹	¹⁴¹ Ce	3.3 x 10 ¹	2.9 x 10 ¹⁰
⁹⁰ Y	1.1 x 10 ⁴	1.2 x 10 ⁹	¹⁴³ Ce	1.4 x 10 ⁰	2.9 x 10 ¹⁰
⁹¹ Y	5.9 x 10 ¹	2.6 x 10 ¹⁰	¹⁴⁴ Ce	2.8 x 10 ⁻²	2.1 x 10 ¹⁰
⁹⁵ Zr	6.4 x 10 ¹	3.1 x 10 ¹⁰	¹⁴⁷ Nd	1.1 x 10 ¹	1.1 x 10 ¹⁰
⁹⁵ Nb	3.5 x 10 ¹	3.0 x 10 ¹⁰	¹⁴⁷ Pm	9.5 x 10 ²	4.2 x 10 ⁹

⁹⁶ Nb	9.8 x 10 ¹	3.1 x 10 ¹⁰	^{148m} Pm	4.1 x 10 ¹	8.5 x 10 ⁹
⁹⁹ Mo	2.7 x 10 ⁰	3.2 x 10 ¹⁰	¹⁴⁹ Nd	2.2 x 10 ⁰	5.8 x 10 ⁹
^{99m} Tc	2.7 x 10 ⁰	2.8 x 10 ¹⁰	¹⁵¹ Pm	1.2 x 10 ⁰	2.6 x 10 ⁹
¹⁰³ Ru	3.9 x 10 ¹	2.0 x 10 ¹⁰	¹⁵¹ Sm	3.3 x 10 ⁴	3.4 x 10 ⁷
¹⁰⁵ Rh	1.5 x 10 ⁰	1.0 x 10 ¹⁰	¹⁵³ Sm	1.9 x 10 ⁰	1.1 x 10 ⁹
¹⁰⁶ Ru	3.7 x 10 ²	4.5 x 10 ⁹	¹⁵⁴ Eu	3.1 x 10 ³	3.7 x 10 ⁷
^{110m} Ag	2.5 x 10 ²	5.3 x 10 ⁸	¹⁵⁵ Eu	1.7 x 10 ³	4.85 x 10 ⁷
¹¹¹ Ag	7.5 x 10 ⁰	4.4 x 10 ⁸	¹⁵⁶ Eu	1.5 x 10 ¹	1.9 x 10 ⁸
^{115m} In	1.9 x 10 ¹	8.6 x 10 ⁷	¹⁶⁰ Tb	7.2 x 10 ¹	1.0 x 10 ⁷
^{117m} Sn	1.4 x 10 ¹	8.3 x 10 ⁷	²³⁷ Np	7.8 x 10 ⁸	1.4 x 10 ³
¹²³ Sn	1.3 x 10 ²	9.9 x 10 ⁷	²³⁹ Np	2.4 x 10 ⁰	3.1 x 10 ¹¹
¹²⁴ I	4.2 x 10 ⁰	1.4 x 10 ⁸	²³⁶ Pu	1.0 x 10 ³	6.0 x 10 ²
¹²⁵ Sb	1.0 x 10 ³	7.8 x 10 ⁷	²³⁸ Pu	3.2 x 10 ⁴	6.8 x 10 ⁶
^{125m} Te	5.8 x 10 ¹	1.6 x 10 ⁷	²³⁹ Pu	8.8 x 10 ⁶	5.0 x 10 ⁶
^{126m} Sb	1.2 x 10 ¹	4.4 x 10 ⁸	²⁴⁰ Pu	2.4 x 10 ⁶	7.8 x 10 ⁶
¹²⁶ Sb	1.2 x 10 ¹	6.1 x 10 ⁷	²⁴¹ Pu	5.1 x 10 ³	9.6 x 10 ⁸
¹²⁷ Sb	3.8 x 10 ⁰	1.1 x 10 ⁹	²⁴² Pu	1.4 x 10 ⁸	1.5 x 10 ⁴
¹²⁷ Te	1.1 x 10 ²	8.9 x 10 ⁸	²⁴¹ Am	1.6 x 10 ⁵	8.7 x 10 ⁵
^{129m} Te	3.3 x 10 ¹	5.5 x 10 ⁹	²⁴³ Am	2.7 x 10 ⁶	5.1 x 10 ⁴
¹³¹ I	8.0 x 10 ⁰	1.6 x 10 ¹⁰	²⁴² Cm	1.6 x 10 ²	2.3 x 10 ⁸
^{131m} Xe	1.2 x 10 ¹	1.8 x 10 ⁸	²⁴⁴ Cm	6.6 x 10 ³	2.2 x 10 ⁶

303

304 A good correlation ($R^2=0.98$) was observed between fallout densities of ⁹⁵Zr (estimated from
305 the activity concentration of daughter product ⁹⁵Nb)¹ and ¹⁴⁴Ce (Figure 7a) because both
306 radionuclides were released and deposited as fuel particles (Kuriny et al., 1993; Kashparov et
307 al., 2003; Kashparov, 2003). The fallout density ratio of ¹⁴⁴Ce/⁹⁵Zr=0.73±0.05, decay corrected
308 to 6th May 1986 was similar to that estimated for Chernobyl reactor fuel (¹⁴⁴Ce/⁹⁵Zr=0.68)
309 (Table 1).

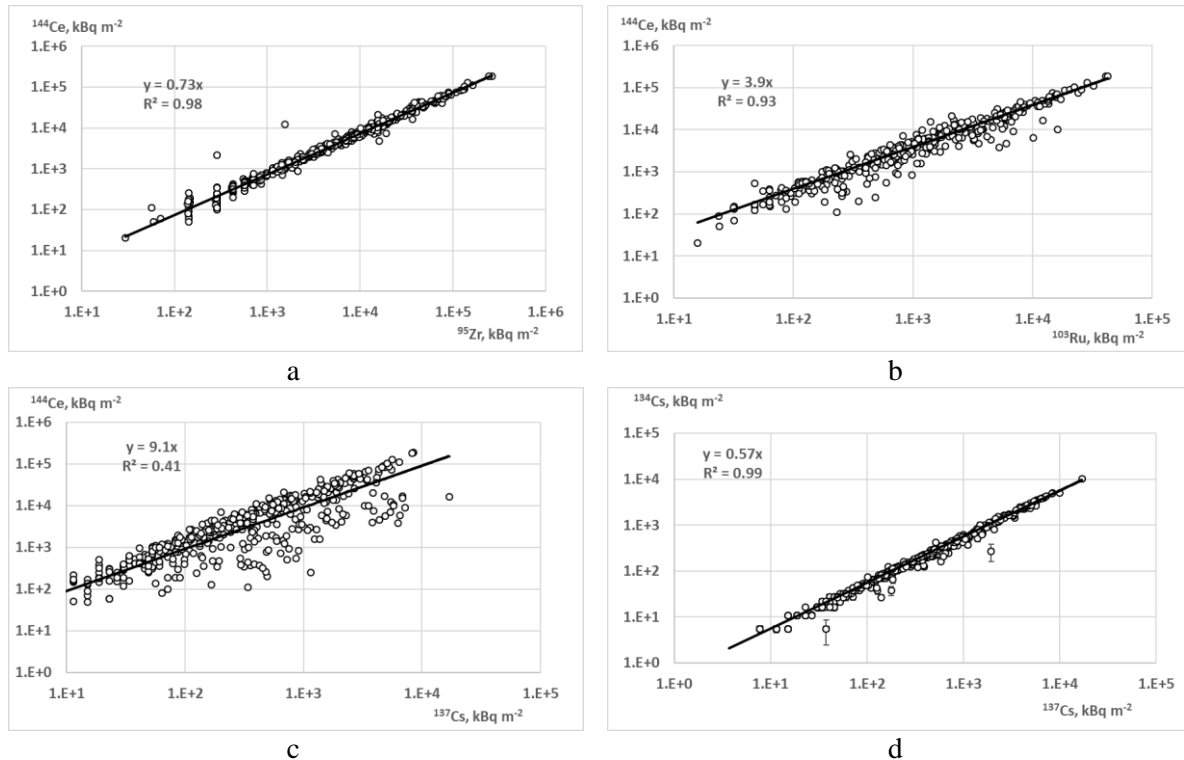
310 The activity ratio of ¹⁴⁴Ce to ¹⁰⁶Ru in fallout was correlated ($R^2=0.93$) and was 3.9±0.4 decay
311 corrected to 6th May 1986 (Figure 7b). The value was close to the ratio of ¹⁴⁴Ce/¹⁰⁶Ru estimated
312 for fuel in the ChNPP number four reactor (4.7) (Table 1). Excess ¹⁰⁶Ru activity relative to
313 ¹⁴⁴Ce activity in some soil samples was observed likely due to the presence of “ruthenium
314 particles” (a matrix of iron group elements with a high content of ^{103,106}Ru (Kuriny et al., 1993;
315 Kashparov et al., 1996)).

316 There was a weak correlation ($R^2=0.41$) between ¹⁴⁴Ce and ¹³⁷Cs activities in the fallout
317 because, as already discussed, caesium was largely deposited as condensation particles while
318 cerium was deposited in fuel particles only. However, in highly contaminated areas close to
319 the ChNPP a significant part of the ¹³⁷Cs was deposited as fuel particles and the activity ratio
320 of ¹⁴⁴Ce/¹³⁷Cs of 9.1 (Figure 7c) broadly corresponded to that of 15 in the reactor fuel (Table
321 1).

¹ Niobium-95 ($T_{1/2}=34$ days) is the daughter radionuclide of ⁹⁵Zr ($T_{1/2}=65$ days) and the ratio of their activities at an equilibrium equals ⁹⁵Nb/⁹⁵Zr=2.1.

322 Different radioisotopes of caesium escaped from nuclear fuel and were deposited in the same
 323 way. This similar behaviour of ^{134}Cs and ^{137}Cs resulted in a strong correlation ($R^2=0.99$)
 324 between their activities in soil samples and the ratio of $^{134}\text{Cs}/^{137}\text{Cs}=0.57\pm 0.07$ was similar to
 325 that estimated for the reactor fuel (0.64, Table 1).

326



327 Figure 7. Correlation between deposition densities of different radionuclides decay corrected
 328 to 6th May 1986.

329

330 3 Use of the data

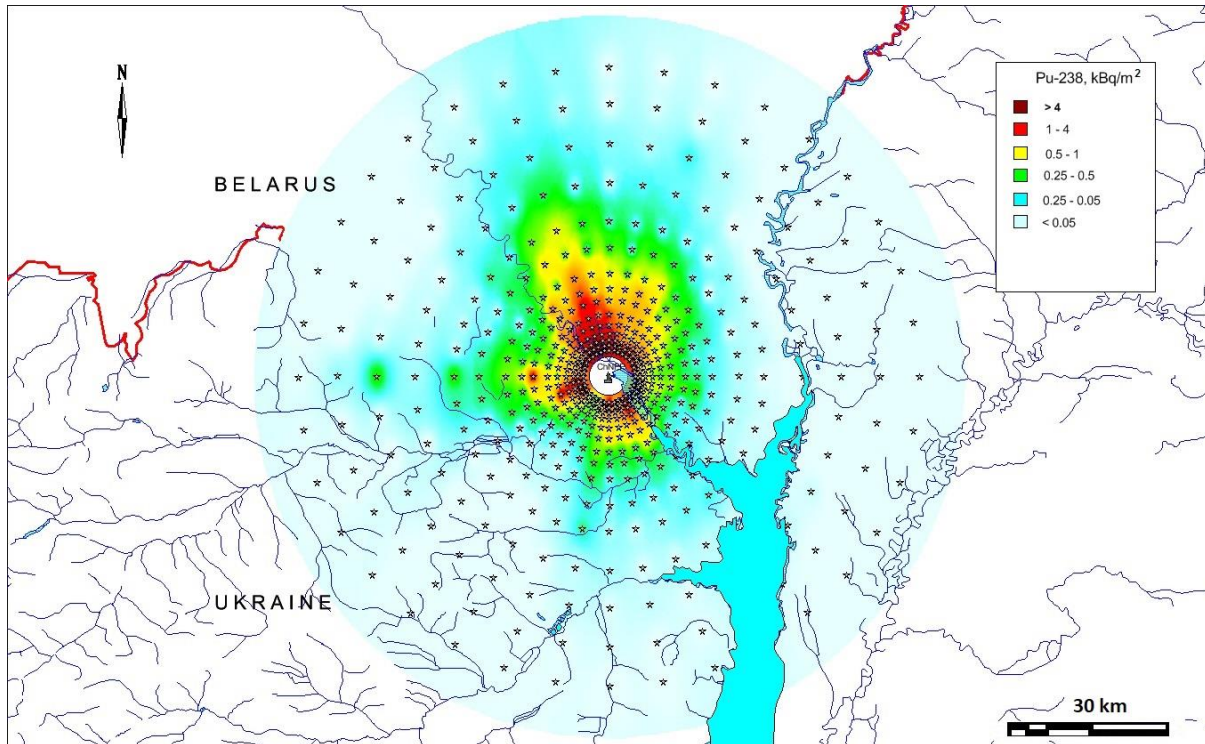
331 Apart from adding to the available data with which contamination maps for the CEZ and
 332 surrounding areas can be generated (e.g. Kashparov et al., 2018) the data discussed in this paper
 333 can be used to make predictions for less well studied radionuclides.

334 The determination of beta and alpha emitting radionuclides in samples requires radiochemical
 335 extraction which is both time consuming and relatively expensive. Large-scale surveys of the
 336 deposition of alpha and beta emitting radionuclides are therefore more difficult than those for
 337 gamma-emitting radionuclides and are not conducive with responding to a large-scale accident
 338 such as that which occurred at Chernobyl. Above we have demonstrated that the deposition
 339 behaviour of different groups of radionuclides was determined by the form in which they were
 340 present in the atmosphere (i.e. associated with fuel particles or condensation particles).

341 We propose that ^{144}Ce deposition can be used as a marker of the deposition of fuel particles;
 342 fuel particles were the main deposition form of nonvolatile radionuclides (i.e. Sr, Y, Nb, Ru,
 343 La, Ce, Eu, Np, Pu, Am, Cm). Therefore, using ^{144}Ce activity concentrations determined in soil
 344 samples and estimates of the activities in reactor fuel, we can make estimates of the deposition
 345 of radionuclides such as Pu-isotopes and Cm that have been relatively less studied. For
 346 example, activity ratios of ^{238}Pu , ^{239}Pu , ^{240}Pu and ^{241}Pu to ^{144}Ce , at the time of measurement

347 would be 8.4×10^{-4} , 6.2×10^{-4} , 9.7×10^{-4} and 1.1×10^{-1} respectively (estimated by decay correcting
 348 data presented in Table 1). Fallout densities of these plutonium isotopes can therefore be
 349 calculated for all sampling points where deposition density of ^{144}Ce was measured either in this
 350 study (e.g. Figure 3) or in other data sets. As an example of the application of the data in this
 351 manner, Figure 8 presents the estimated deposition of ^{238}Pu ; Figure 8 was prepared using the
 352 TIN (triangulated irregular network) interpolation within MAPINFO. The first maps of ^{90}Sr
 353 and $^{239+240}\text{Pu}$ surface contamination from the Chernobyl accident were prepared in the frame
 354 of an international project (IAEA, 1992) in a similar way.

355



356

357 Figure 8. The fallout density of ^{238}Pu (kBq m^{-2}) corrected to 6th May 1986; estimated from
 358 measurements of ^{144}Ce in soil and estimated activity concentrations in the fuel of the ChNPP
 359 reactor number four (note no data were available for less than 5 km from ChNPP and no
 360 interpolation for this area has been attempted).

361

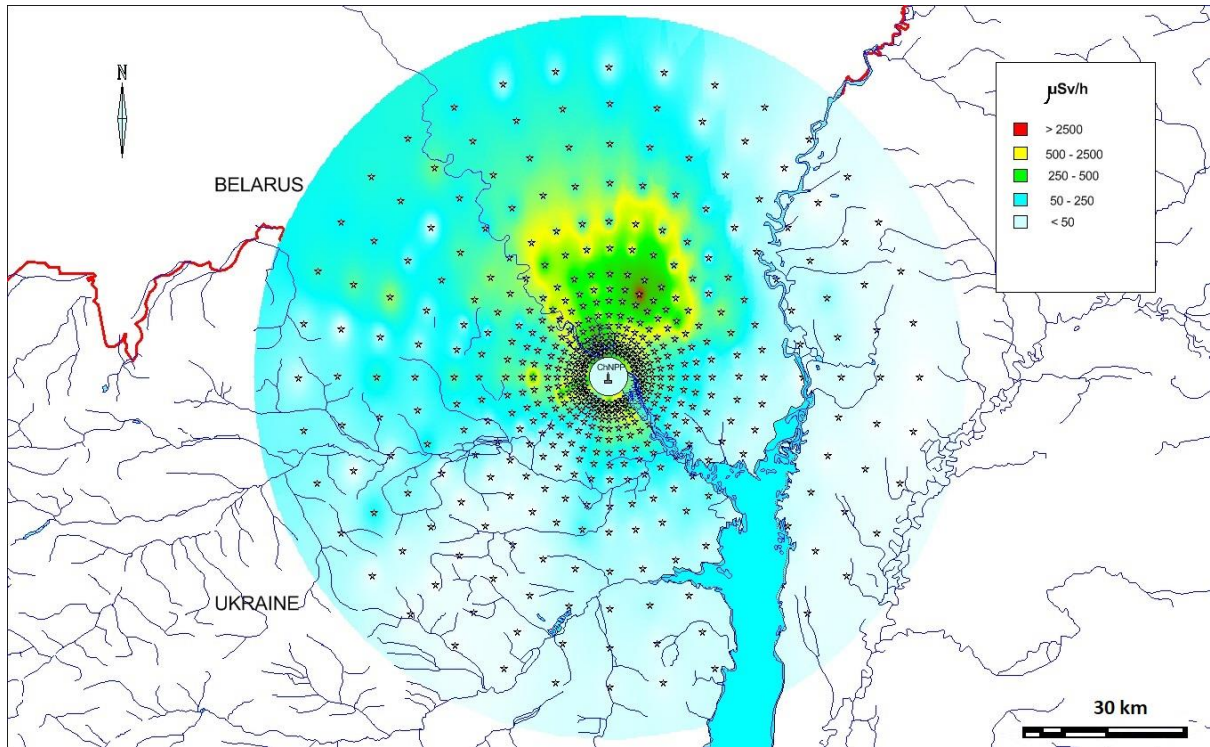
362 The dynamic spatial distribution of gamma dose rate can be reconstructed using the data on
 363 radionuclide contamination densities (Kashparov et al., 2019) in combination with the ratios
 364 between activities of radionuclides in fuel and in condensed components of Chernobyl fallout
 365 (Table 1) and also dose coefficients for exposure to contaminated ground surfaces, ($\text{Sv s}^{-1}/\text{Bq}$
 366 m^{-2}) (Eckerman & Ryman, 1993). Five days after deposition the following radionuclides were
 367 major contributors (about 95 %) to gamma dose rate: ^{136}Cs , ^{140}La , ^{239}Np , ^{95}Nb , ^{95}Zr , ^{131}I , $^{148\text{m}}\text{Pm}$,
 368 ^{103}Ru , ^{140}Ba , ^{132}Te . After three months the major external dose contributors were: ^{95}Nb ,
 369 ^{95}Zr , $^{148\text{m}}\text{Pm}$, ^{134}Cs , ^{103}Ru , $^{137\text{m}}\text{Ba}$, $^{110\text{m}}\text{Ag}$, ^{136}Cs , ^{106}Rh . Three years after the major contributors
 370 were $^{137\text{m}}\text{Ba}$, ^{134}Cs , ^{106}Rh , $^{110\text{m}}\text{Ag}$, ^{154}Eu . At the present time the gamma dose can be estimated
 371 to be mainly (99%) due to the gamma-emitting daughter radionuclide of ^{137}Cs ($^{137\text{m}}\text{Ba}$). Bondar
 372 (2015) from a survey of the CEZ along the Ukrainian-Belarussian border, showed a good
 373 relationship between ^{137}Cs contamination ($A_{\text{Cs-137}}$, in the range of 17-7790 kBq m^{-2}) and

374 ambient dose rates at 1m above the ground (D_{ext} , in the range of 0.1-6.0 $\mu\text{Sv h}^{-1}$). The
375 relationship was described by following equation with correlation coefficient of 0.99:

376
$$D_{ext} = 0.0009 \cdot A_{Cs-137} + 0.14.$$

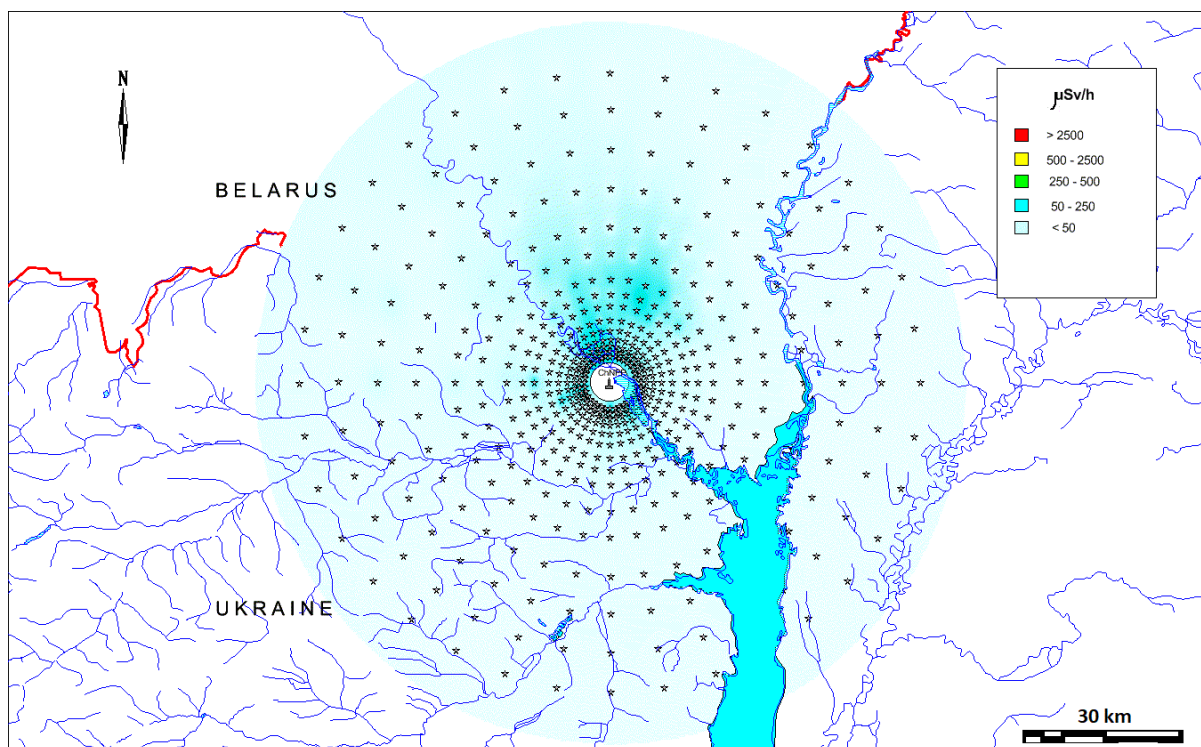
377 As an example of the application of the data in this manner, Figure 9 presents the estimated
378 external effective gamma dose rate five and 95 days after the cessation of the radioactive
379 releases from the reactor on 6th May 1986.

380



382

a



383

384

b

385 Figure 9. Spatial distribution, interpolated as for Figure 8, of effective dose rate within the 60
 386 km zone around the ChNPP on 10th May 1986 (a) and 10th August 1986 (b). Note no data
 387 were available for less than 5 km from ChNPP and no interpolation for this area has been
 388 attempted.

389 The estimated effective dose rate values exceed the evacuation dose criteria of 50 $\mu\text{Sv h}^{-1}$ over
 390 a large area (especially in the north and west) of the 60 km area around the ChNPP on 10th May
 391 1986 (Figure 9a); as discussed above a dose rate of 50 $\mu\text{Sv h}^{-1}$ on 10th May 1986 equated to a
 392 total dose over the first year after the accident of 50 mSv - the value used to define areas for
 393 evacuation. On the 10th August 1986 the area estimated to exceed 50 $\mu\text{Sv h}^{-1}$ was restricted to
 394 the north (Figure 9b). The dose rate decreased quickly after the accident due to the radioactive
 395 decay of short-lived radionuclides. The dominance of these short-lived radionuclides and a lack
 396 of knowledge of the radionuclide composition of the fallout made it difficult in 1986 to estimate
 397 external dose rates to the public for an evaluation date of 10th May 1986 (most dose rate
 398 measurements being made after the 10th May). This likely resulted in the overestimation of
 399 dose rates for some villages in 1986 leading to their evacuation when the external dose rate
 400 would not have been in excess of the 50 mSv limit used by the authorities.

401 There is a need for deposition data for the CEZ and surrounding areas for a number of reasons.
 402 These include exploring risks associated with future management options for the CEZ (e.g.
 403 management of the water table, forest fire prevention, increased tourism, etc.) and also the
 404 return of abandoned areas outside of the CEZ to productive use. The long-term effect of
 405 radiation exposure on wildlife in the CEZ is an issue of much debate (e.g. see discussion in
 406 Beresford et al., 2019). Improved data which can be used to map the contamination of a range
 407 of radionuclides will be useful in improving dose assessments to wildlife (including
 408 retrospective assessments of earlier exposure rates). The CEZ has been declared a
 409 'Radioecological Observatory' (Muikku et al., 2018) (where a Radioecology Observatory is
 410 defined as a radioactively contaminated field site that provides a focus for joint, long-term,

411 radioecological research). The open provision of data as described in this paper fosters the spirit
412 of collaboration and openness required to make the observatory site concept successful and
413 joins a growing amount of data made available for the CEZ (Kashparov et al., 2017; Fuller et
414 al., 2018; Kendrick et al., 2018; Gaschak et al., 2018; Beresford et al., 2018; Lerebours and
415 Smith, 2019).

416

417 **4 Data availability**

418 The data described here have a digital object identifier (doi: 10.5285/a408ac9d-763e-4f4c-
419 ba72-73bc2d1f596d) and are freely available for registered users from the NERC
420 Environmental Information Data Centre (<http://eidc.ceh.ac.uk/>) under the terms of the Open
421 Government Licence (Kashparov et al., 2019).

422 Competing interests. The authors declare that they have no conflict of interest.

423 Acknowledgements. Funding for UKCEH staff to contribute to preparing this paper and the
424 accompanying data set (Kashparov et al., 2019) was provided by the TREE project
425 (<http://www.ceh.ac.uk/tree>; funded by NERC, the Environment Agency and Radioactive
426 Waste Management Ltd under the RATE programme) and associated iCLEAR
427 (<https://tree.ceh.ac.uk/content/iclear-0>; funded by NERC) projects.

428 Author contribution. Soil samples were collected by the USSR Ministry of Defence and
429 delivered to UIAR. Sample preparation, analysis and data interpretation was carried out by
430 UIAR staff contributing as follows: Kashparov, Levchuk, Protsak, - sample preparation,
431 measurement of radionuclide activity concentrations in samples; Kashparov - analysis of
432 results; Zhurba - database creation and preparation of the manuscript figures (maps). The
433 manuscript was prepared by Chaplow, Beresford, Kashparov, Levchuk and Zhurba.

434

435 **References**

436 Aleksakhin, R.M., Buldakov, L.A., Gubanov, V.A., Drozhko, E.G., Ilyin, L.A., Kryshev, I.I., Linge, I.I., Romanov, G.N.,
437 Savkin, M. N., Saurov, M.M., Tikhomirov, F.A., Kholina, Yu.B. Major radiation accidents: consequences and protective
438 measures. Edited by L.A. Ilyin and V.A. Gubina. book published in Moscow, Publishing House Izdat. 752 p. (data from p.
439 481). ISBN 5-86656-113-1. http://elib.biblioatom.ru/text/krupnye-radiatsionnye-avarii_2001/go/0/, 2001.

440 Begichev, S. N., Borovoy, A.A., Burlakov, E.V., Gavrilov, S.L., Dovbenko, A.A., Levina, L.A., Markushev, V.M.,
441 Marchenko, A.E., Stroganov, A.A., Tataurov, A.L. Preprint IAE-5268/3: Reactor Fuel of Unit 4 of the Chernobyl NPP (a
442 brief handbook). Kurchatov In st. Atomic Energy, 1990.

443 Beresford, N.A., Gaschak, S., Barnett, C.L., Maksimenko, A., Guliaichenko, E., Wells, C., Chaplow, J.S. A 'Reference Site'
444 in the Chernobyl Exclusion Zone: radionuclide and stable element data, and estimated dose rates NERC-Environmental
445 Information Data Centre. <https://doi.org/10.5285/ae02f4e8-9486-4b47-93ef-e49dd9ddec4>, 2018.

446 Beresford, N.A., Scott, E.M., Coppstone, D. Field effects studies in the Chernobyl Exclusion Zone: Lessons to be learnt J.
447 Environ. Radioact. <https://doi.org/10.1016/j.jenvrad.2019.01.005>, 2019

448 Bondar Yu. Field studies in the Chernobyl exclusion zone along the Belarusian border (dosimetric monitoring and soil
449 radiation analysis). Report of Polesye State Radiation and Ecological Reserve. Belarus, Khoiniki, 2015.

450 Chaplow, J. S., Beresford, N. A., and Barnett, C. L.: Post-Chernobyl surveys of radiocaesium in soil, vegetation, wildlife and
451 fungi in Great Britain, Earth Syst. Sci. Data, 7, 215–221, <https://doi.org/10.5194/essd-7-215-2015>, 2015.

452 De Cort, M., Dubois, G., Fridman, Sh. D., Germenchuk, M. G., Izrael, Yu. A., Janssens, A., Jones, A. R., Kelly, G. N.,
453 Kvasnikova, E. V., Matveenko, I., Nazarov, I. M., Pokumeiko, Yu. M., Sitak, V. A., Stukin, E. D., Tabachny, L. Ya.,
454 Tsaturov, Yu. S., and Avdyushin, S. I.: Atlas of caesium deposition on Europe after the Chernobyl accident, Luxembourg,
455 Office for Official Publications of the European Communities, ISBN 92-828-3140-X, 1998.

456 Eckerman K.F. and Ryman J.C. External exposure to radionuclides in air, water, and soil. Federal guidance report No. 12,
457 EPA-402-R-93-081, Oak Ridge National Laboratory, Tennessee 37831, USA, 238 P., 1993.

458 Fuller, N., Smith, J.T., Ford, A.T. Effects of low-dose ionising radiation on reproduction and DNA damage in marine and
459 freshwater amphipod crustaceans. NERC Environmental Information Data Centre. [https://doi.org/10.5285/b70afb8f-0a2b-](https://doi.org/10.5285/b70afb8f-0a2b-40e6-aecc-ce484256bbfb)
460 [40e6-aecc-ce484256bbfb](https://doi.org/10.5285/b70afb8f-0a2b-40e6-aecc-ce484256bbfb), 2018.

461 Gaschak, S.P., Beresford, N.A., Barnett, C.L.; Wells, C., Maksimenko, A., Chaplow, J.S. 2018 Radionuclide data for
462 vertebrates in the Chernobyl Exclusion Zone NERC-Environmental Information Data Centre.
463 <https://doi.org/10.5285/518f88df-bfe7-442e-97ad-922b5aef003a>, 2018.

464 Hilpert K., Odoj R., and Nurnberg H. W. Mass spectrometric study of the potential of Al₂O₃/SiO₂ additives for the retention
465 of cesium in coated particles. Nucl. Technol., 61: 71, 1983.

466 IAEA. International Chernobyl Project: Technical Report. International Advisory Committee. Vienna, 1991.

467 IAEA. International Chernobyl project, technical report. ISBN 92-0-400192-5 ([http://www-](http://www-pub.iaea.org/MTCD/publications/PDF/Pub886_web/Start.pdf)
468 [pub.iaea.org/MTCD/publications/PDF/Pub886_web/Start.pdf](http://www-pub.iaea.org/MTCD/publications/PDF/Pub886_web/Start.pdf)), 1992.

469 IAEA. Environmental consequences of the Chernobyl accident and their remediation: twenty years of experience. Report of
470 the Chernobyl Forum Expert Group "Environment" (eds. L. Anspaugh and M. Balonov). Radiological assessment reports
471 series, IAEA, STI/PUB/1239, 166 pp., 2006.

472 IAEA. Guidelines on soil and vegetation sampling for radiological monitoring. Technical Reports Series No. 486.
473 International Atomic Energy Agency. Vienna, 247p. [https://www.iaea.org/publications/12219/guidelines-on-soil-and-](https://www.iaea.org/publications/12219/guidelines-on-soil-and-vegetation-sampling-for-radiological-monitoring)
474 [vegetation-sampling-for-radiological-monitoring](https://www.iaea.org/publications/12219/guidelines-on-soil-and-vegetation-sampling-for-radiological-monitoring). 2019.

475 Izrael, Yu.A., Vakulovsky, S.M., Vetrov, V.A., Petrov, V.N., Rovinsky, F.Ya., Stukin, E.D.. Chernobyl: Radioactive
476 Contamination of the Environment. Gidrometeoizdat publishers, Leningrad, 223 pp. 1990 (in Russian).

477 Kashparov, V. A.: Hot Particles at Chernobyl, Environ. Sci. Pollut. R., 10, 21–30, 2003.

478 Kashparov, V. A., Ivanov, Y. A., Zvarich, S. I., Protsak, V. P., Khomutinin, Y. V., Kurepin, A. D., and Pazukhin, E. M.:
479 Formation of Hot Particles During the Chernobyl Nuclear Power Plant Accident, Nucl. Technol., 114, 246–253, 1996.

480 Kashparov, V.A.; Lundin, S.M.; Zvarich, S.I.; Yoschenko, V.I.; Levchuk, S.E., Khomutinin, Yu.V., Maloshtan, I.N.,
481 Protsak, V.P. Territory contamination with the radionuclides representing the fuel component of Chernobyl fallout. The
482 Science of the Total Environment. 317(1-3), 105-119. [https://doi.org/10.1016/S0048-9697\(03\)00336-X](https://doi.org/10.1016/S0048-9697(03)00336-X), 2003.

483 Kashparov, V., Levchuk, S., Zhurba, M., Protsak, V., Khomutinin, Y., Beresford, N. A., and Chaplow, J. S.: Spatial datasets
484 of radionuclide contamination in the Ukrainian Chernobyl Exclusion Zone, NERC-Environmental Information Data Centre,
485 <https://doi.org/10.5285/782ec845-2135-4698-8881-b38823e533bf>, 2017.

486 Kashparov, V.; Levchuk, S.; Zhurba, M.; Protsak, V.; Khomutinin, Yu.; Beresford, N.A.; Chaplow, J.S. Spatial datasets of
487 radionuclide contamination in the Ukrainian Chernobyl Exclusion Zone. Earth System Science Data (ESSD). 10, 339-353.
488 <https://doi.org/10.5194/essd-10-339-2018>, 2018.

489 Kashparov, V.; Levchuk, S.; Zhurba, M.; Protsak, V.; Beresford, N.A.; Chaplow, J.S. Spatial radionuclide deposition data
490 from the 60 km radial area around the Chernobyl nuclear power plant, 1987. NERC Environmental Information Data Centre.
491 <https://doi.org/10.5285/a408ac9d-763e-4f4c-ba72-73bc2d1f596d>, 2019.

492 Kendrick, P., Barçante, L., Beresford, N.A., Gashchak, S., Wood, M.D. Bird Vocalisation Activity (BiVA) database:
493 annotated soundscapes from the Chernobyl Exclusion Zone. NERC Environmental Information Data Centre.
494 <https://doi.org/10.5285/be5639e9-75e9-4aa3-afdd-65ba80352591>, 2018.

495 Kuriny, V. D., Ivanov, Y. A., Kashparov, V. A., Loschilov, N. A., Protsak, V. P., Yudin, E. B., Zhurba, M. A., and
496 Parshakov, A. E.: Particle associated Chernobyl fall-out in the local and intermediate zones, Ann. Nucl. Energy, 20, 415–
497 420, 1993.

498 Lerebours, A., Smith, J.T.. Water chemistry of seven lakes in Belarus and Ukraine 2014 to 2016. NERC Environmental
499 Information Data Centre. <https://doi.org/10.5285/b29d8ab8-9aa7-4f63-a03d-4ed176c32bf3>, 2019.

500 Loshchilov, N. A., Kashparov, V. A., Yudin, Y. B., Protsak, V. P., Zhurba, M. A., and Parshakov, A. E.: Experimental
501 assessment of radioactive fallout from the Chernobyl accident, Sicurezza e Protezione, 25–26, 46–49, 1991.

502 Muikku, M., Beresford, N.A., Garnier-Leplice, J., Real, A., Sirkka, L., Thorne, M., Vandenhove, H., Willrodt, C.
503 Sustainability and integration of radioecology—position paper J. Radiol. Prot. 38, 152-163,
504 <http://iopscience.iop.org/article/10.1088/1361-6498/aa9c0b>, 2018.

505 National Report of Ukraine. Twenty-five Years after Chernobyl Accident: Safety for the Future. – K.: KIM. – 328 p., 2011.

506 Pontillon, Y; Ducros, G; Malgouyres, P.P. 2010. Behaviour of fission products under severe PWR accident conditions
507 VERCORS experimental programme—Part 1: General description of the programme. Nuclear Engineering and Design.
508 240(7), 1843–1852 <https://doi.org/10.1016/j.nucengdes.2009.06.028>, 2010.

509 Saji G. A scoping study on the environmental releases from the Chernobyl accident (part I): Fuel particles. American
510 Nuclear Society International Topical Meeting on Probabilistic Safety Analysis, PSA 05: 685-696, 2005.

511 Salbu, B., Krekling, T., Oughton, D.H., Ostby, G., Kashparov, V.A., Brand, T.L., Day, J.P. Hot Particles in Accidental
512 Releases from Chernobyl and Windscale Nuclear Installations. Analyst 119: 125-130, 1994.

513 Talerko N.. Mesoscale modelling of radioactive contamination formation in Ukraine caused by the Chernobyl accident. J. of
514 Env. Radioactivity. – 78: 311-329, 2005

515 UIAR: The map of the 30-km Chernobyl zone terrestrial density of contamination with cesium-137 (in 1997), UIAR, Kyiv,
516 Ukraine, 1998.

517 United Nations Scientific Committee on the Effects of Atomic Radiation, UNSCEAR, Sources and effects of ionizing
518 radiation. Report to the General Assembly with Scientific Annexes, volume II, Annex D. Health effects due to radiation
519 from the Chernobyl accident. United Nations, New York, 178 pp., 2008.

520
521
522
523
524
525
526
527
528
529
530
531
532
533
534
535
536
537
538
539
540
541
542
543
544
545
546
547
548
549
550